

DETC2003/PTG-48006

INFLUENCE OF SHOT PEENING ON SURFACE DURABILITY OF PLASMA CASE-HARDENED SINTERED POWDER METAL GEARS

Akira YOSHIDA Dept. of Mechanical Engineering, Okayama University
 3-1-1, Tsushima-Naka, Okayama, 700-8530, JAPAN
 Tel +81-86-251-8034, Fax +81-86-251-8266, E-mail: akira-y@mech.okayama-u.ac.jp

Yuji OHUE Dept. of IMSE, Kagawa University
 2217-20, Hayashi-cho, Takamatsu, 761-0396, JAPAN
 Tel +81-87-864-2344, Fax +81-87-864-2369, E-mail: ohue@eng.kagawa-u.ac.jp

Masanori SEKI Dept. of Mechanical Engineering, Okayama University
 3-1-1, Tsushima-Naka, Okayama, 700-8530, JAPAN
 Tel +81-86-251-8036, Fax +81-86-251-8266, E-mail: seki@mech.okayama-u.ac.jp

ABSTRACT

In order to investigate the influence of shot peening on the surface durability of sintered powder metal gears, the plasma case-hardened sintered powder metal rollers and gears shot-peened with different condition were fatigue-tested under a sliding-rolling contact condition.

The hardness, the compressive residual stress and the surface roughness of the rollers and gears increased by the shot peening. The failure mode of the rollers and gears was mainly spalling. The main crack of the failed rollers and gears propagated through the pores below the roller and the tooth surfaces. The surface durabilities of the lightly shot-peened rollers and gears were higher than those of the other rollers and gears. While, the surface durabilities of the strongly shot-peened rollers are lower than that of the unpeened roller because of the increase of the surface roughness and the deformed sharp pore by the strong shot peening.

Key word: *Gear, Sintered Material, Shot Peening, Plasma Case Hardening, Surface Durability*

INTRODUCTION

The rolling contact machine parts, such as gears, bearings, cams and so on, made by powder metallurgy are widely used as the machine elements. However, compared with the machine elements made of melted steel, those of sintered powder metals have a disadvantage in the fatigue strength because of their pores. Therefore, in this study, the test rollers and test gears made of sintered powder metals were shot-peened under several conditions after plasma case hardening, and those were fatigue-tested to investigate the influence of shot peening con-

dition on the surface durability of those, for improving the fatigue strength.

TEST ROLLERS AND TEST GEARS

The manufacturing conditions of plasma case-hardened sintered powder metal rollers and gears are given in Table 1. The partially alloyed metal powder with particle diameters from 127 μ m to 175 μ m was mixed with graphite and zinc stearate, and was compacted into discs. The green density of these discs was 6.9g/cm³. After the compacting, these discs were sintered in N₂ gas.

The shapes and dimensions of test roller pair are shown in

Table 1 Manufacturing conditions of test rollers and test gears

Powder type	0.7% Mn, 1.0% Cr 0.2% Mo, Balance Fe	
Particle diameter	127 μ m to 175 μ m	
Mixing	0.3% Graphite 0.8% Zinc stearate	
Compacting pressure	64 kN/cm ²	
Green density	6.9 g/cm ³	
Sintering	1403K x 0.5hr, in N ₂ gas	
Machining	Turning (Roller) Hobbing, Turning (Gear)	
Finishing	Grinding	
Plasma case-hardening	Temperature	1223 K
	Heating time	2.7 hr
	Atmospheric pressure	533Pa, H ₂ : C ₃ H ₈ = 3 : 2

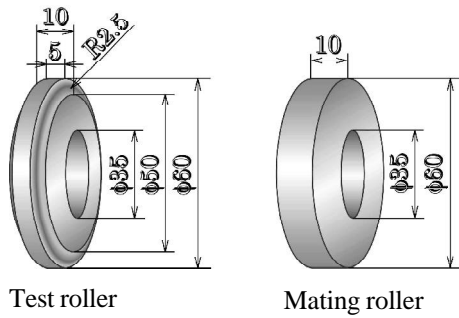


Fig.1 Shapes and dimensions of test roller pair

Table 2 Specification of test gear pair

		Pinion	Gear
Module	mm	5	
Pressure angle	deg.	20	
Number of teeth		15	16
Addendum modification coefficient		0.571	0.560
Tip circle diameter	mm	90.71	94.60
Center distance	mm	82.55	
Facewidth	mm	18	6
Contact ratio		1.246	
Accuracy*		Class 4	Class 4
Tooth surface finishing		Grinding	

*JIS B 1702

Fig.1. The test roller pair with 60mm in diameter was used in this study. The above discs were machined to the test roller with 60mm in diameter by turning, and then they were finish-ground. Finally, the circumferential surfaces of those were plasma case-hardened and shot-peened.

The specification of test gear pair is given in Table 2. Spur gear pair was used in this study. The gear pair had involute profile teeth, a module of 5mm, a standard pressure angle of 20deg. and a contact ratio of 1.246. The above discs were machined to the gear by turning and hobbing, and then they were finish-ground. Lastly, the tooth surfaces of those were plasma case-hardened and shot-peened. Mating rollers and mating pinions made of chromium molybdenum steel (JIS:SCM415) were finish-ground after case hardening.

The shot peening conditions, the surface roughness and the surface hardness of test rollers and test gears are given in Table 3 and Table 4, respectively. The surface roughnesses of test rollers were measured along the axial direction of them, and those of test gears were measured along the tooth profile direction of them. The specimen marks R and G represent unpeened roller and unpeened gear, respectively. The other specimen marks including letters R and G represent shot-peened rollers and shot-peened gears, respectively. Test roller RD0.6 and test gear GD0.6, which are reference roller and gear, were shot-peened with steel shot having a diameter of 0.6mm and a hardness of 620HV at a velocity of 60m/s for 200sec. The other test rollers and gears were marked by the shot peening conditions under different shot velocity, shot diameter and shot hardness. The same specimen marks except letters R and G represent the roller and gear shot-peened under same condition. Concerning the

Table 3 Shot peening conditions of test rollers

Specimen mark	Roller				
	R	RV30H	RD0.2	RH520	RD0.6
Shot velocity	m/s	---	30	60	
Shot diameter	mm	---	0.2		0.6
Shot hardness	HV	---	520	620	520 620
Peening time	sec	---	200		
Projection amount	N/min	---	980		
Arc height	mmA	---	0.085	0.190	0.360 0.520
Coverage	%	---	1000	2000	480 600
Surface roughness	Ry μ m	0.8	7.9	7.5	10.1 12.7
Surface hardness	HV	735	810	822	820 850

Table 4 Shot peening conditions of test gears

Specimen mark	Gear				
	G	GD0.2	GH520	GD0.6	GD0.8
Shot velocity	m/s	---	60		
Shot diameter	mm	---	0.2	0.6	0.8
Shot hardness	HV	---	620	520	620
Peening time	sec	---	200		
Projection amount	N/min	---	980		
Arc height	mmA	---	0.190	0.360	0.520 0.640
Coverage	%	---	800	430	550 360
Surface roughness	Ry μ m	3.2	5.4	7.5	11.2 14.1
Surface hardness	HV	710	750	800	827 850

arc height value [1] which is one of the indexes showing the shot peening intensity, the larger arc height value is, the stronger shot peening is, generally. Thus, there is a tendency that the surface roughness and the surface hardness of test rollers and test gears increased as the arc height value increased. It can be understood, from the results of the test rollers and test gears shot-peened under same condition, the surface roughness and the surface hardness of test rollers are larger than those of test gears. The coverage value [2] is the percentage of the shot impression area to the shot-peened area. The coverage values of test rollers are also larger than those of test gears. The surface roughness and the surface hardness of mating roller were 1.4 μ m and 840HV, and those of mating pinion were 3.2 μ m and 800HV, respectively.

Figure 2 shows the average hardness distributions of test rollers and test gears. The Vickers hardness was measured with a microhardness tester under a measuring load of 0.98N for 30sec. The average hardness distribution was obtained from five measured hardnesses at each depth below the surface. The measured hardnesses were scattered within a range of \pm 50HV from the average hardness. The hardnesses of test gears were measured at the working pitch point along the normal direction to the tooth surface. As shown in Fig.2, the hardnesses of all test rollers and gears were almost similar to each other over a depth of 0.5mm below the surface. However, the hardness near the surface increased by the shot peening. The effective case-hardened depths, where the hardness is 550HV, were 1.1mm to 1.2mm for the test rollers, and were 0.9mm to 1.1mm for the test gears. The effective case-hardened depths of mating roller and mating pinion were about 1.0mm and about 0.8mm, respectively.

The residual stress distributions of test rollers are shown

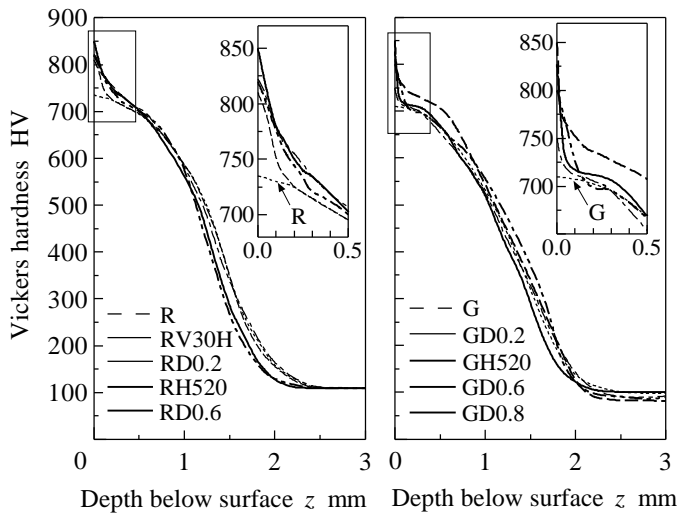


Fig.2 Hardness distributions of test rollers and test gears

in Fig.3. The residual stresses were measured according to the $2\theta\text{-sin}^2\psi$ method [3] using $\text{CrK}\alpha$ -ray as characteristic X-ray. For the stress analysis below the contact roller surface, an arbitrary point at the center of the roller surface was chosen as the origin, and the x , y and z coordinates were taken in the axial, circumferential and radial directions of the roller, respectively. The surface layer of the roller was removed by electrolytic polishing to measure the residual stress below the roller surface. The residual stresses $(\sigma_x)_r$ and $(\sigma_y)_r$ in the axial and the circumferential directions of the roller, shown in Fig.3, were determined by modifying the measured residual stresses by the elastic calculation [4], since the measured stresses were influenced by the removal of the surface layer. The residual stress $(\sigma_z)_r$ in the radial direction of the roller was determined by the elastic equations [4]. The residual stresses $(\sigma_x)_r$ and $(\sigma_y)_r$ of the shot-peened rollers were in compressive field in the surface layer. These compressive residual stresses were larger than those of the unpeened roller R. The surface residual stresses of test rollers and test gears are given in Table 5. In the case of the gear, the residual stresses $(\sigma_x)_r$ and $(\sigma_y)_r$ were measured in the tooth trace and the tooth profile directions of the gear, respectively. In this study, compared with the residual stresses $(\sigma_x)_r$ and $(\sigma_y)_r$ of test rollers, those of test gears were hardly influenced by the shot peening.

The Young's modulus and the Poisson's ratio of test rollers and test gears are 152GPa and 0.25, and those of mating rollers and mating pinions are 206GPa and 0.30, respectively.

The surface profiles of test rollers and test gears are shown in Fig.4. The surface profiles of test rollers were measured along the axial direction of them, and those of test gears were measured along the tooth profile direction of them, in the same manner as at measuring the surface roughness. In the surface profiles of the unpeened roller R and gear G, the grinding marks can be observed. On the other hand, in the surface profiles of the other rollers and gears, the grinding marks disappeared by the shot peening. Additionally, the stronger shot peening was, the rougher surface profiles of the shot-peened rollers and gears were. Especially, the larger shot diameter caused the rougher surface profiles of shot-peened rollers and gears.

Figure 5 shows the cross sections of test rollers and test gears below the surface by a metallurgical microscope. The

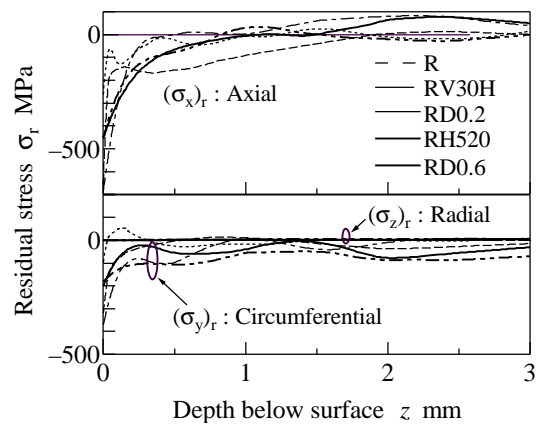


Fig.3 Residual stress distributions of test rollers

Table 5 Surface residual stresses of test rollers and test gears

Specimen mark	Roller				
	R	RV30H	RD0.2	RH520	RD0.6
$(\sigma_x)_r$ MPa	-262	-650	-686	-456	-450
$(\sigma_y)_r$ MPa	-95	-320	-370	-181	-210
Specimen mark	Gear				
	G	GD0.2	GH520	GD0.6	GD0.8
$(\sigma_x)_r$ MPa	-304	-403	-387	-244	-331
$(\sigma_y)_r$ MPa	-338	-378	-363	-265	-302

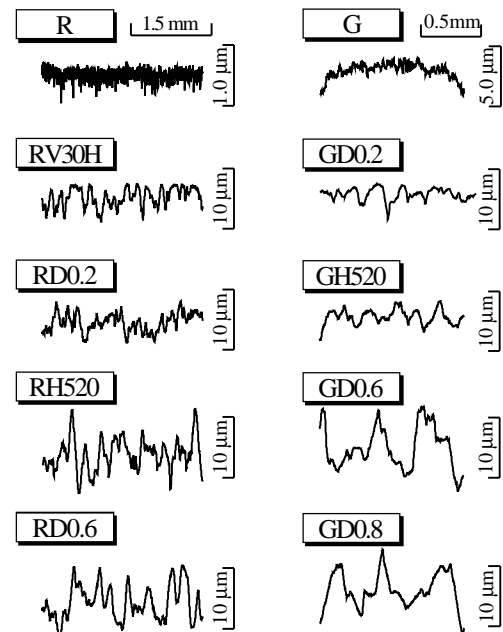


Fig.4 Surface profiles of test rollers and test gears

black spots in this figure indicate the pores below the roller surface and the tooth surface. The pores of the unpeened roller R were distributed uniformly below the roller surface. However, the pores near the surface of the shot-peened rollers and gears were deformed except those of the shot-peened gear GD0.2. The tendency that the pores near the surface of the shot-peened gear GD0.2 was not deformed compared with those of the shot-peened roller RD0.2 is similar to that the surface roughnesses

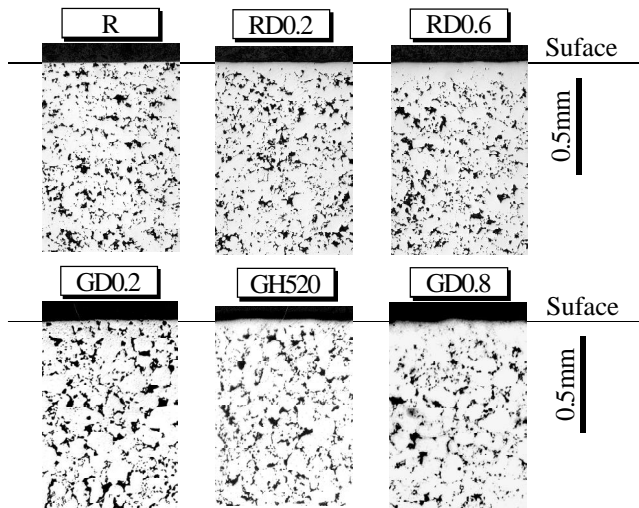


Fig.5 Cross sections of test rollers and test gears

of shot-peened gears are smaller than those of shot-peened rollers under same shot peening condition. These may be due to the difference between the coverage values of test rollers and test gears under same shot peening condition.

EXPERIMENTAL PROCEDURES

The rolling contact fatigue tests of the rollers were performed using a spring-loading type two cylinder testing machine [5]. The relative radius of curvature in the roller pair with 60mm diameter was 15mm. The load between the test roller and the mating roller given by a compression spring could be detected by the strain gauges put on the tension bar. The maximum Hertzian stress p_{max} [6] was adopted as the standard of the loading between contact rollers. These roller tests were performed under the operating conditions given in Table 6. The test rollers were taken as the slower rollers, and the mating rollers were taken as the faster rollers.

The operating fatigue tests of the gears were performed at a rotational speed of test gear of 1800rpm using a power circulating type gear testing machine [7], that is, IAE type gear testing machine with a center distance of 82.55mm. In this test gear pair, the maximum of the relative radius of curvature was 9.71mm in tooth meshing, and the tangential velocity at the working pitch point on the tooth surfaces of the test gear and the mating pinion was 3.78m/s. The test gears were used as the driven gears in this experiment. The specific sliding on the tooth surface of test gear changed +66 percent to -200 percent during tooth meshing. The load between the test gear and the mating pinion was given by a load lever and weights. The maximum Hertzian stress p_{max} [8] at working pitch point was adopted as the standard of the loading for the tooth meshing of test gear pair.

The lubricating oil employed in both the roller tests and the gear tests was EP gear oil whose properties are given in Table 7. This lubricating oil contains the extreme pressure additives, and was pressure supplied to the engaging side of the roller pair and the gear pair from nozzles. The flow rate of the supplied oil was about 1500ml/min for the roller pair and about 750ml/min for the gear pair. The oil temperature was adjusted to 313±4K.

In this study, the minimum oil film thickness by D.Dowson [9] was in the range of 2.4μm to 2.6μm for the test roller pair and in the range of 1.2μm to 2.2μm for the test gear pair. While, the

Table 6 Operating conditions of test rollers

Testing machine type	φ60
Rotational speed of slower roller	1432 rpm
Circumferential velocity of slower roller	4.50 m/s
Rotational speed of faster roller	1800 rpm
Circumferential velocity of faster roller	5.65 m/s
Specific slinding of slower roller	-25.7 %
Specific slinding of faster roller	+20.4 %
Slinding velocity	1.15 m/s

Table 7 Property of lubricating oil

Specific gravity	288/277K	0.9022
Flash point	K	477
Pour point	K	260.5
Kinematic viscosity x10 ⁻⁶ m ² /s	313K	190.9
	373K	17.74
Viscosity index		98
Total acid number	mgKOH/g	2.26

D value defined by P.H.Dawson [10] was above 1 for all the roller pairs and all the gear pairs except the case of the test roller R. In the calculation of the minimum oil film thickness and the D value, the oil temperatures between the operating surfaces were taken as 313K, which is supplied oil temperature, in both the roller test and the gear test.

SURFACE DURABILITY

Figure 6 shows the relationships between the maximum Hertzian stress p_{max} and the number of cycles to failure N , that is, the p_{max} - N curves obtained by the rolling contact fatigue tests of the rollers and the operating fatigue tests of the gears. The roller testing machine and the gear testing machine were automatically stopped when the vibration transducers fixed on the machines acted by the vibration increase due to the surface failure or the tooth breakage. The fatigue life of test rollers and test gears was defined as the total number of cycles when the testing machine was automatically stopped. The fatigue life of test gears, in addition, was defined as the total number of cycles when the percentage of pitted area in a test gear pair reached 5 percent. The spalled area on the tooth surface was also considered as the pitted area. These p_{max} - N curves were determined by the method of least squares using the experimental plots of the fatigue life under each Hertzian stress. The arrows in this figure indicate that no fatal surface failure occurred on the roller and the tooth over 2×10^7 cycles. In this study, the fatigue limit of the test roller and the test gear, that is, the surface durability of them was defined as the maximum Hertzian stress at 2×10^7 cycles. The surface durabilities of the test rollers RH520 and RD0.6, which were shot-peened with 0.6mm diameter shots at a shot velocity of 60m/s, are lower than that of the unpeened roller R. On the other hand, those of the test rollers RV30H and RD0.2, which were shot-peened with 0.2mm diameter shots, are higher than that of the unpeened roller R. In the case of test gears, those of all shot-peened gears are higher than that of the unpeened gear G.

The relationships between the arc height value, i.e., the shot peening intensity and the surface durability are shown in

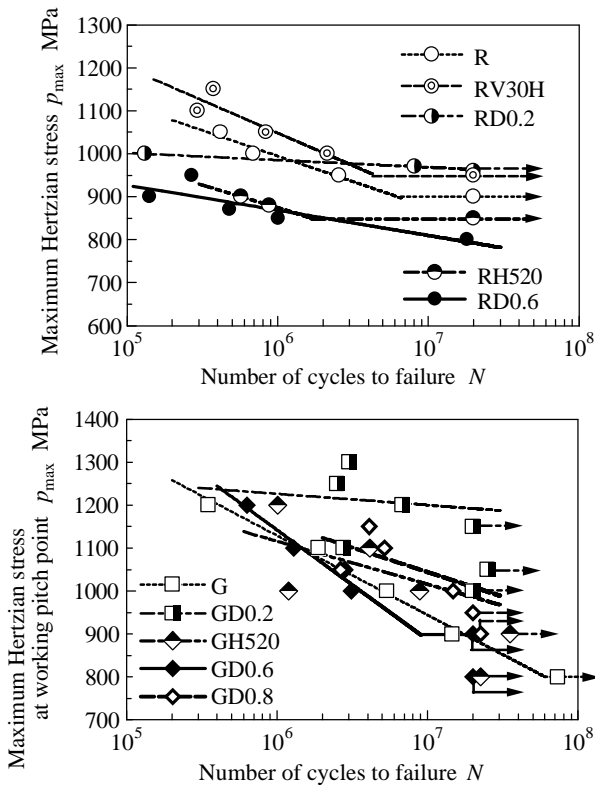


Fig.6 p_{max} - N curves

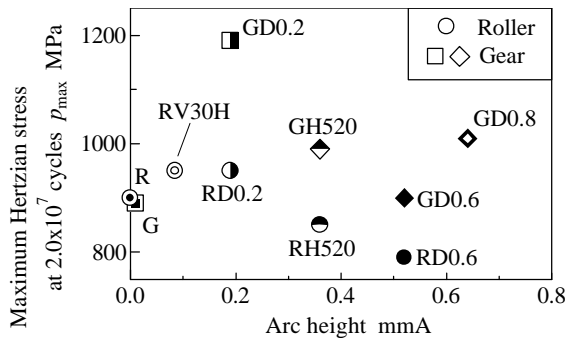


Fig.7 Relation between surface durability and arc height value

Fig.6 for each test roller and gear. It can be understood from this figure that the surface durabilities of the test rollers RV30H and RD0.2 are the highest in test rollers, and those of the test gear GD0.2 is also the highest in test gears. Therefore, it can be considered that such lightly shot peening condition as applied to RV30H, RD0.2 and GD0.2 is good for improving the surface durabilities of the sintered powder metal rollers and gears. By the way, the surface durability of sintered powder metal rollers decreased as the relative radius of curvature increased in the past experiment [11]. As above, the relative radius of curvature of the test roller pair is about one and a half as large as that of the test gear pair. Moreover, the surface durabilities of the lightly shot-peened rollers and gears are higher than those of the strongly shot-peened rollers and gears as shown in Fig.7. Compared with the surface roughness of test gears, that of test rollers was influenced by the shot peening as shown in Table 3 and Table 4. Thus, it follows from these that as for the surface durabilities of test rollers and test gears shot-peened under same condition, the surface durabilities of test rollers are lower

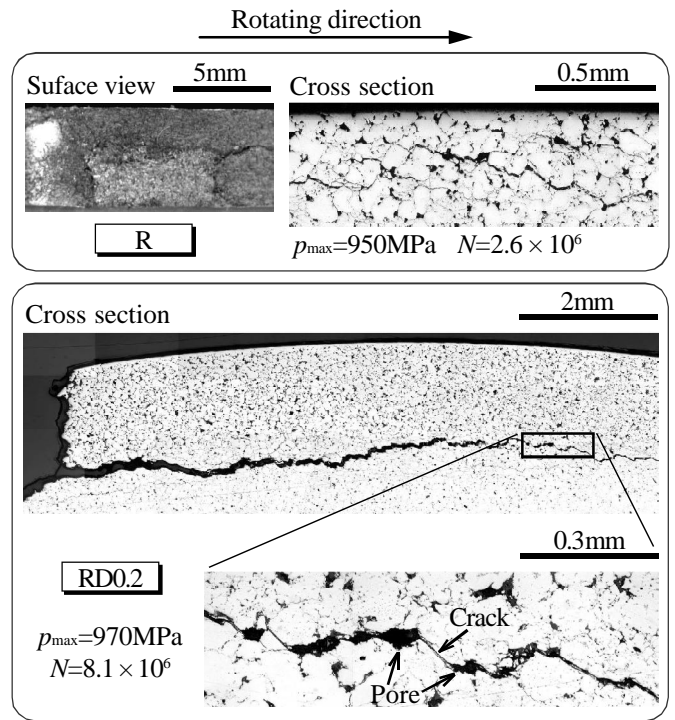


Fig.8 Observation of failed rollers

than those of test gears.

FAILURE MODE

Figure 8 shows the surface and the transverse section of the failed rollers. All test rollers were failed near the case-core boundary at a depth of about 2mm below the roller surface, except both cases of the roller R tested under $p_{max}=950\text{MPa}$ and the roller RV30H tested under $p_{max}=1150\text{MPa}$ which were failed near the roller surface. It can be observed in Fig.8 that the main cracks of the failed rollers propagated below and almost parallel to the roller surface. In a magnified photograph taken from a part near the main crack, a fine crack connecting one pore to another pore can be observed. From these observations, it can be said that the failure mode of the test rollers in this study was spalling due to subsurface cracking. The reason why the rollers R and RV30H were occasionally failed near the roller surface within the hardened layer is that the work hardening by the lightly shot peening was less effective than that by the strongly shot peening.

Figure 9 shows the appearances of the failed teeth and an example of the transverse section of failed tooth in the test gear GD0.2 tested under $p_{max}=1100\text{MPa}$. The micropits on the dedendum flanks of only the test gears G and GD0.2 occurred at the early stage of the fatigue process, as shown in the photograph (A). The failure mode of the test gear G was the pitting, which occurred on the dedendum flanks as shown in the photograph (B), except for the failure mode of the test gear G tested under $p_{max}=1200\text{MPa}$ which was the tooth breakage due to bending fatigue at the tooth fillet. The failure mode of the shot-peened gears was the spalling, which finally occurred due to the separation from the tooth surface. In the photograph (C), the subsurface spalling crack which propagated almost parallel to the tooth surface below the dedendum flank can be observed. It can be considered that the pitting on the tooth surface of shot-peened gears occurred hardly because of the increase of the surface hardness and the compressive residual stress by

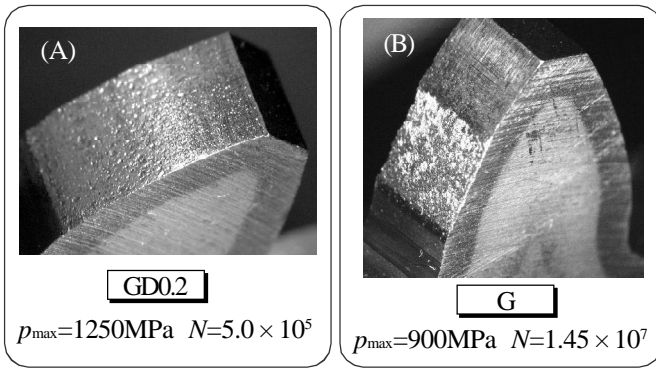


Fig.9 Observation of failed teeth

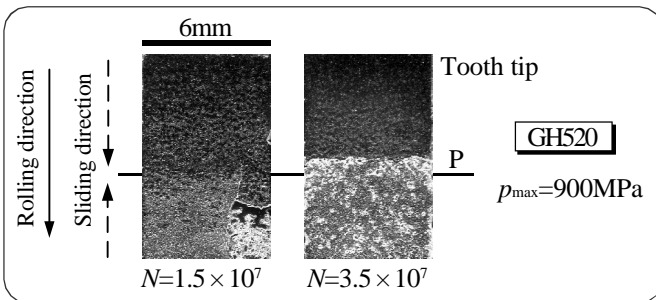
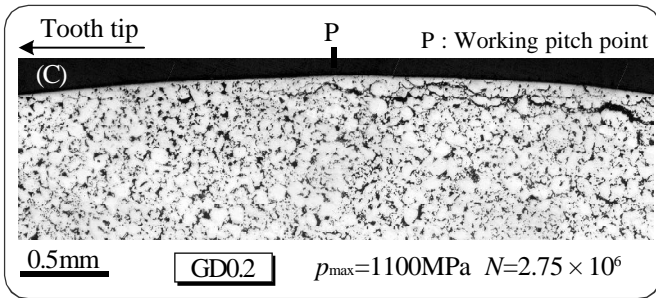


Fig.10 Failed tooth surface of test gear

the shot peening. The replica observation on the failed tooth of the test gear GH520 tested under $p_{max}=900\text{MPa}$ is shown in Fig.10. It could be observed from this figure that the separation on part of the dedendum flank occurred, and then it spread over the whole dedendum flank. All the spalling cracks of the shot-peened gears occurred in a range of the tooth surface to a depth of 0.5mm, that is, near the tooth surface, except for the spalling cracks on the tooth side of some test gears appeared at a depth of about 1.2mm from the tooth surface as shown in Fig.11. These spalling cracks as shown in Fig.11 did not become the fatal failure for the gears in this experiment.

DISCUSSION OF EXPERIMENTAL RESULTS BY AMPLITUDE OF RATIO OF SHEAR STRESS TO VICKERS HARDNESS

In the case of the case-hardened melted steel rollers [5,12] and gears [13], the occurring depth of the spalling crack depended on the depth where the amplitude $A(t/HV)$ of the ratio of shear stress t to Vickers hardness HV became peak. In this experiment, the spalling crack could be observed for both test rollers and gears. Therefore, the same theory using the amplitude of the ratio of shear stress to Vickers hardness was also applied to the plasma case-hardened sintered powder metal rollers and gears in this paper. Alternating orthogonal shear stress t_{yz} and pulsating maximum shear stress t_{45° were considered

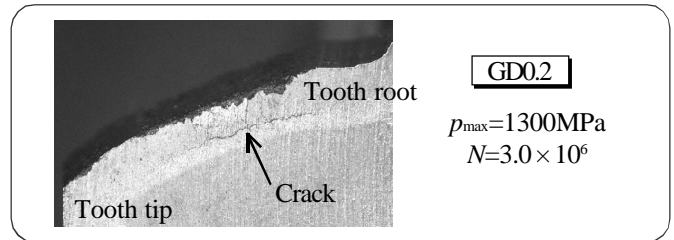


Fig.11 Spalling crack of test gear

here. In the calculations of these shear stresses on and below the contact surface, the contact point on the roller surface or the tooth surface was chosen as the origin, the x coordinate was taken in the axial direction of the roller or the tooth trace direction of the gear, y coordinate in the circumferential direction of the roller or the tooth profile direction of the gear and z coordinate in the radial direction of the roller or the normal direction to the tooth surface of the gear. These shear stresses on and below the contact surface were calculated using the analytical method by J.O.Smith [14] obtained for the uniform continuous body. The amplitude $A(t/HV)$ of the ratio of shear stress to Vickers hardness was also calculated by neglecting the effect of mean stress on fatigue and by assuming that the material strengths of the test rollers and test gears are proportional to the average hardnesses of those rollers and gears [5]. For calculating this amplitude $A(t/HV)$, the hardness distribution and the residual stress distribution of test rollers were considered in the case of the test rollers, and only the hardness distribution of test gears was considered in the case of the test gears.

Some examples of the calculated distributions of the amplitudes $A(t/HV)$ for test rollers and test gears are shown in Fig.12. The distributions of the amplitude $A(t/HV)$ for all the test rollers and gears are in similar shape. In the cases of all the test rollers and gears, the amplitude $A(t_{yz}/HV)$ values of the ratio of orthogonal shear stress t_{yz} to Vickers hardness HV is larger than the amplitude $A(t_{45^\circ}/HV)$ values of the ratio of maximum shear stress t_{45° to Vickers hardness HV. Generally, the fatigue life becomes shorter as the amplitude becomes larger. Therefore, it can be considered that the spalling failure and the surface durability are much more influenced by the amplitude $A(t_{yz}/HV)$ than by the amplitude $A(t_{45^\circ}/HV)$. For this reason, the relationship between the amplitude $A(t_{yz}/HV)$ and the failure depth of test roller and test gear was studied in this study. The distributions of the amplitude $A(t_{yz}/HV)$ for test rollers and test gears have two peaks at the shallower depth within the hardened layer and at the deeper depth near the case-core boundary. The former was denoted as $[A(t_{yz}/HV)]_{peak1}$, the latter was denoted as $[A(t_{yz}/HV)]_{peak2}$. The maximum of the amplitude $A(t_{yz}/HV)$ is the peak amplitude $[A(t_{yz}/HV)]_{peak2}$ for the test rollers, and the depth where the peak amplitude $[A(t_{yz}/HV)]_{peak2}$ is located agreed with the depth where most of the test rollers were failed. In the case of the test gears, the maximum of the amplitude $A(t_{yz}/HV)$ is the peak amplitude $[A(t_{yz}/HV)]_{peak1}$ or $[A(t_{yz}/HV)]_{peak2}$ case by case. In the past paper [11], it was obtained that the gradient of the amplitude distribution near the surface became steeper as the relative radius of curvature decreased. Thus, it follows from this and Fig.12 that the gradient of the amplitude distribution near the surface in the case of test gears is steeper than that in the case of test rollers, since the relative radius of curvature in

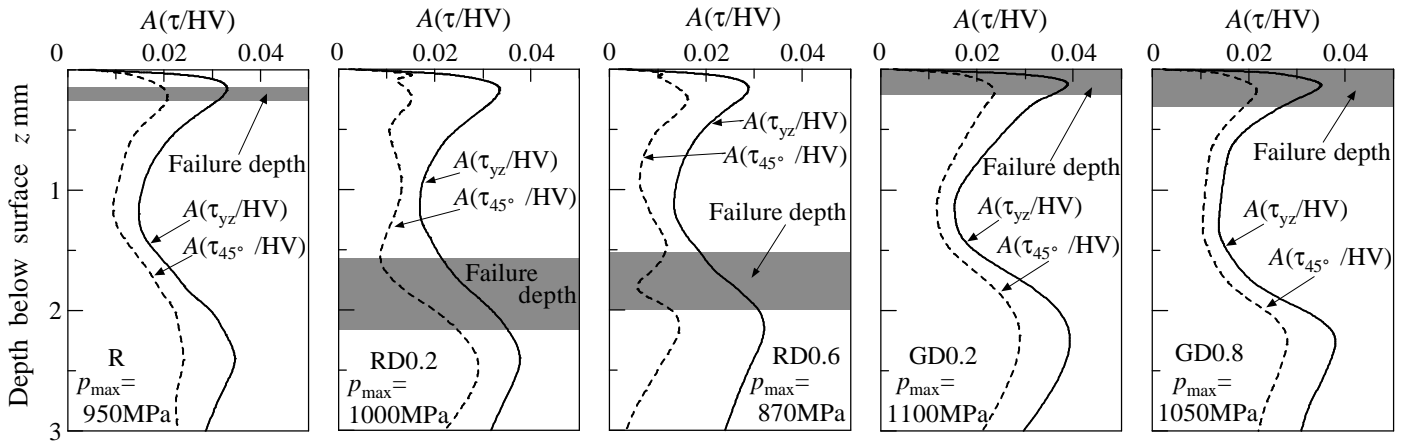


Fig.12 Distributions of $A(t/HV)$

the test gear pair is smaller than that in the test roller pair in this study. As mentioned above, additionally, the effect of the shot peening on the test gears was less than that on the test rollers under same shot peening condition. For these reasons, it can be considered that all the test gears were failed near the depth where the peak amplitude $[A(t_{yz}/HV)]_{peak1}$ is located, that is, near the tooth surface. Generally, the friction coefficient between the rollers becomes large as the surface roughness of the rollers increases. Consequently, the shear stress below the contact surface of the rollers increases, since the increase of the friction coefficient between the rollers results into the increase of the tangential force between those [15]. The same understanding as mentioned above can be obtained in the case of the gears. While, as shown in Fig.5, the pores near the surface of the strongly shot-peened rollers and gears were deformed heavily. Generally, the stress concentration factor becomes larger as the radius of curvature of a notch becomes smaller [16]. Compared with the undeformed pore, the incidence of crack at the pore deformed by shot peening becomes higher due to the stress concentration at the end of the deformed pore. Thus, the spalling crack became easy to be initiated from the sharp notch of the pores deformed near the surface of the shot-peened rollers and gears. Therefore, it could be said that the strongly shot-peened rollers and gears became easy to be failed due to the increase of the surface roughness and the sharp deformed pore.

Figure 13 shows the relationships between the peak amplitude $[A(t_{yz}/HV)]_{peak}$ and the number of cycles to failure N , i.e., the $[A(t_{yz}/HV)]_{peak}-N$ curves, where the maximum Hertzian stress p_{max} in the ordinates of Fig.6 were exchanged for the peak amplitude $[A(t_{yz}/HV)]_{peak}$. The peak amplitudes $[A(t_{yz}/HV)]_{peak}$ in this figure were used as the peak amplitude $[A(t_{yz}/HV)]_{peak1}$ or $[A(t_{yz}/HV)]_{peak2}$ which is located near the failure depth for each test roller and gear. Specifically, the peak amplitudes $[A(t_{yz}/HV)]_{peak}$ of the test rollers R tested under $p_{max}=950\text{MPa}$ and RV30H tested under $p_{max}=1150\text{MPa}$, which were failed near the roller surface, were used as the peak amplitude $[A(t_{yz}/HV)]_{peak1}$. Those of the other test rollers, which were failed at a depth of about 2mm below the roller surface, were used as the peak amplitude $[A(t_{yz}/HV)]_{peak2}$. In the case of test gears, those were used as the peak amplitude $[A(t_{yz}/HV)]_{peak1}$, since all the test gears were failed near the tooth surface, except for a case that the failure mode of the test gear G under $p_{max}=1200\text{MPa}$ was tooth breakage. As mentioned above, the failure depth of test rollers and test gears is related to the amplitude $A(t_{yz}/HV)$. Thus,

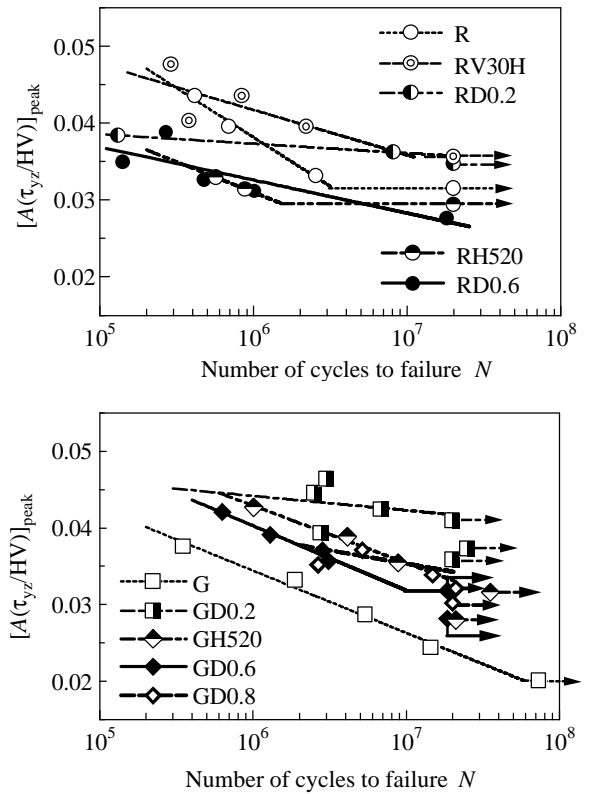


Fig.13 $[A(t_{yz}/HV)]_{peak}-N$ curves

it could be considered that the peak amplitude $[A(t_{yz}/HV)]_{peak}$ located near the failure depth of test rollers and test gears is possible to be adopted as the standard for the spalling failure and the surface durability of those.

In the case of the rollers, the $[A(t_{yz}/HV)]_{peak}-N$ curves of the lightly shot-peened rollers are higher than that of the unpeened roller R, and those of the strongly shot-peened rollers are lower. These tendencies indicate that the effect of the surface roughness and the deformed sharp pore on the life of the rollers appears, since the effect of the hardness is eliminated. In the case of the gears, the same understanding as mentioned above can be obtained. The dispersion of the plots of the shot-peened gears in Fig.13 is smaller than that in Fig.6, additionally in Fig.13 the plots of all the shot-peened gears are higher than those of the unpeened gear G. It can be said that the surface roughness and the deformed sharp pore of the gears influenced hardly on

the surface durability of those, but the residual stress of those influenced. As for the rollers and the gears shot-peened under same condition, besides, the $[A(t_{yz}/HV)]_{\text{peak}}-N$ curves of the gears are higher than those of the rollers, since the relative radius of curvature and the coverage value of the gears are smaller than those of the rollers. Therefore, it may be possible to evaluate the fatigue life and the surface durability of the gears, using the $[A(t_{yz}/HV)]_{\text{peak}}-N$ curves of the rollers. It could be followed, lastly, that the light shot peening, which does not cause too large surface roughness and the sharp deformed pore, has to be selected in order to improve the surface durability of plasma case-hardened sintered powder metal gears.

CONCLUSION

In order to investigate the influence of shot peening on the surface durability of sintered powder metal gears, the plasma case-hardened sintered powder metal rollers shot-peened under four different conditions were fatigue-tested under a sliding-rolling contact condition, and the plasma case-hardened sintered powder metal spur gears shot-peened under four different conditions were also fatigue-tested using a power circulating type gear testing machine. The following points can be concluded from this study.

1. The hardness, the compressive residual stress and the roughness of the rollers and gears increased by the shot peening. The pores near the surface of those were deformed by shot peening, except for the case of the lightly shot-peened gear GD0.2 in this experimental range.
2. The failure mode of the rollers and gears was spalling, excepting a case of the unpeened gear where the pitting occurred. The failure depth of the rollers and gears agreed almost with the depth where the amplitude $A(t_{yz}/HV)$ of the ratio of orthogonal shear stress to Vickers hardness became peak.
3. In the case of the rollers, only the surface durabilities of the lightly shot-peened rollers, such as RV30H and RD0.2, were higher than that of the unpeened roller. In the case of the gears, the surface durabilities of all the shot-peened gears were higher than that of the unpeened gear, especially, that of the lightly shot-peened gear GD0.2 was highest.
4. Judging from the $p_{\text{max}}-N$ curves and also the $[A(t_{yz}/HV)]_{\text{peak}}-N$ curves, it is proposed that the light shot peening, which does not cause too large surface roughness and the deformed sharp pore, has to be selected in order to improve the surface durability of sintered gears.

ACKNOWLEDGMENT

The authors would like to thank Mitsubishi Heavy Industries Limited and Shintokogio Limited for plasma case hardening and shot peening, respectively. Japan Energy Corporation is also thanked for providing the lubricating oil. The authors also thank Mr. Kazuhiko Hagiwara of Okayama University for

his helps. This research was supported financially in part by the Scientific Research Fund of The Japanese Ministry of Education, Culture, Sports, Science and Technology to which the authors express their gratitude.

REFERENCES

- [1] The Shot Peening Technology Association, 1997, *Technique and Effect of Shot Peening* (in Japanese), The Nikkan Kogyo Shinbun, LTD., Tokyo, pp.112.
- [2] *ibid.*, pp.118.
- [3] J.Soc.Mater.Sci.Jpn., 1982, *Standard Method for X-ray Stress Measurement*, J.Soc.Mater.Sci.Jpn., Tokyo, pp.4.
- [4] Shigeru Yonetani, 1944, "On the Method of Measurement of Residual Stress in a Hollow Cylinder by X-Ray Method" (in Japanese), J.Soc.Mater.Sci.Jpn., **18-90**, pp.610-614.
- [5] K.Fujita, A.Yoshida, T.Yamamoto and T.Yamada, 1977, "The Surface Durability of the Case-hardened Nickel Chromium Steel and Its Optimum Case Depth", Bulletin of the JSME, **20-140**, pp.232-239.
- [6] K.L.Johnson, 1987, *Contact Mechanics*, Cambridge University Press, NY, pp.84.
- [7] M.FUJII, F.OBATA, A.YOSHIDA and H.MATSUDA, 1989, "Effect of Tooth Profile on Scoring Behavior in Spur Gears", JSME International Journal, Series III, **32-4**, pp.645-653.
- [8] Darle W.Dudley, 1962, *Gear Handbook*, Mcgraw-hill Book Company, NY, pp.13-18
- [9] D.Dowson, 1967, "Elastohydrodynamics", Proc.Instn. Mech.Engrs., **182-3A**, pp.151-167.
- [10] P.H.Dawson, 1965, "Further Experiments on the Effect of Metallic Contact on the Pitting of Lubricated Rolling Surfaces", Proc.Instn.Mech.Engrs., **180-3B**, pp.95-100.
- [11] A.YOSHIDA, Y.OHUE and I.KARASUNO, 1994, "Surface Failure and Durability of Induction-Hardened Sintered Powder Metal Rollers and Gears with Various Hardened Depths", Transactions of the ASME, **116**, pp.730-737.
- [12] K.FUJITA and A.YOSHIDA, 1978, "Surface Durability of Steel Rollers (In The Case of Case-Hardened and of Nitrided Rollers)", Bulletin of the JSME, **21-154**, pp.761-767.
- [13] A.YOSHIDA, 1989, "Some problems in Design of Surface-Hardened Gears for Tooth Surface Durability", JSME International Journal, Series III, **32-3**, pp.356-364.
- [14] J.O.Smith and C.K.Liu, U.III, 1953, "Stresses Due to Tangential and Normal Loads on an Elastic Solid With Application to Some Contact Stress Problems", Transactions of ASME, **20-2**, pp.157-166.
- [15] A.YOSHIDA, D.KONISHI and M.SAITO, 1991, "Study on Influences of Machining Method and Surface Roughness on Pitting of Thermally Refined Steel Rollers (2nd Report)", J.J.Soc.Tribo., **36-6**, pp.665-676.
- [16] J.Soc.Mater.Sci.Jpn., 1994, *Strength and Fracture of Materials* (in Japanese), J.Soc.Mater.Sci.Jpn., Tokyo, pp.98.